0026-895X/99/060970-12$3.00/0

MOLECULAR PHARMACOLOGY, **55:**970–981 (1999).

Activation and Ca^{2+} Permeation of Stably Transfected $\alpha3/\beta4$ Neuronal Nicotinic Acetylcholine Receptor

J. ZHANG, Y. XIAO, G. ABDRAKHMANOVA, W. WANG, L. CLEEMANN, K.J. KELLAR, and M. MORAD

Department of Pharmacology, Georgetown University School of Medicine, Washington, D.C.

Received November 4, 1998; accepted March 15, 1999

This paper is available online at http://www.molpharm.org

ABSTRACT

The $\alpha3/\beta4$ rat neuronal nicotinic acetylcholine receptor, stably transfected in human embryonic kidney cells, was examined using the whole-cell-clamp technique and 2-dimensional confocal imaging. Application of agonists (nicotine, cytisine, epibatidine) activated a large (100–200 pA/pF) inwardly rectifying monovalent current, with little current at voltages between 0 and +40 mV. Rapid application of nicotine and cytisine indicated EC_{50} values of $\cong$22 and $\cong$64 μM, respectively, and suggested second order binding kinetics (Hill coefficient $\sim$2). The time constant of desensitization (decay) of nicotine-activated current was concentration-dependent (typically $\sim$10 s at 30 μM versus $\sim$1.0 s at 100–1000 μM), but not voltage-dependent and was significantly smaller than the $\sim$200 s reported for the $\alpha3/\beta4$ receptor expressed in *Xenopus* oocytes. Nicotine-activated current was rapidly and reversibly blocked by coapplication of mecamylamine and *d*-tubocurarine. At −80 mV holding potentials, the current was also suppressed by $\sim$25% either upon complete removal or elevation of Ca^{2+} to 10 mM. Total replacement of Na^+ by Ca^{2+} also completely blocked the current. On the other hand, evidence for permeation of Ca^{2+} was indicated by increased inward current at −40 mV upon elevation of Ca^{2+} from 2 to 10 mM, as well as a rise in the cytosolic Ca^{2+} proportional to the current carried by the receptor. These findings are consistent with the idea that Ca^{2+}, in addition to its channel-permeating properties, may also regulate the receptor from an extracellular site. Our results suggest that the $\alpha3/\beta4$ neuronal nicotinic acetylcholine receptor, when stably expressed in human embryonic kidney 293 cells, has desensitization kinetics and Ca^{2+} regulatory mechanisms somewhat different from those described for the receptor expressed in *Xenopus* oocytes.

Neuronal nicotinic acetylcholine receptors (nAChRs) composed of α and β subunits are differentially expressed in the nervous system and constitute a family of ligand-gated cationic channels. Eight α ($\alpha2$–$\alpha9$) and three β ($\beta2$–$\beta4$) neuronal subunit genes have been cloned in chicks, rodents, and humans, consistent with the idea that neurons may express nAChR with a variety of subunit combinations (see McGehee and Role, 1995; Lindstrom, 1996, for recent reviews).

The central nervous system expresses mRNA for all of the nAChR subunits. The receptors that contain the $\alpha3$ subunit, although lower in abundance than $\alpha4$, may mediate important effects of acetylcholine and nicotine in the brain (Connolly et al., 1995) and possibly in the spinal cord. Compared with $\alpha4/\beta2$ receptors, nAChR containing $\alpha3$ subunits appear to have much lower affinity for most nicotinic agonists in the central nervous system (Albuquerque et al., 1997).

The nAChR comprised of $\alpha3$ subunits in combination with either $\beta2$ or $\beta4$ subunits may be the predominant nicotinic receptor in the mammalian sympathetic, parasympathetic, and trigeminal ganglia, and in adrenal chromaffin cells (Nooney and Feltz, 1995). Rat and chicken superior cervical ganglion, chick ciliary ganglion, and PC12 cells also express mRNA for designated $\alpha3$, $\alpha5$, $\beta2$, and $\beta4$ subunits (McGehee and Role, 1995).

Expression studies in *Xenopus* oocytes have shown that functional neuronal nAChRs can be formed by pairwise coinjection of one kind of α and one kind of β subunit (Boulter et al., 1987). The receptor forms with an apparent subunit stoichiometry of two α and three β (Anand et al., 1991) or, in some cases ($\alpha7$ and $\alpha8$), as homomeric assemblies (Séguéla et al., 1993). Both α and β subunits contribute to the pharmacological and biophysical properties of these receptors, giving each subunit combination unique characteristics (Wada et al., 1988; Luetje and Patrick, 1991).

In this report we explore the biophysical and pharmacological characteristics of the $\alpha3/\beta4$ nAChR subtype in a stably transfected mammalian human embryonic kidney (HEK) 293 cell line recently developed in our laboratory (Xiao et al., 1998). Our results suggest that $\alpha3/\beta4$-transfected cells generate a rapidly activating, voltage-dependent monovalent current on exposure to nicotinic receptor agonists. The current shows characteristic inward rectification, desensitization, kinetics, and pharmacology similar but not identical with the neuronal nAChR in chromaffin cells. The electro-

Supported by National Institutes of Health Grants HL16152 and DA06486.

ABBREVIATIONS: nAChR, nicotinic acetylcholine receptor; Ach, acetylcholine; HEK, human embryonic kidney; *d*-tc, *d*-tubocuraine.

physiological and confocal Ca^{2+} imaging data suggest that Ca^{2+} may both permeate and allosterically regulate the α3/β4 receptor (Lena and Changeux, 1993).

Experimental Procedures

Materials. Stably transfected HEK 293 (ATCC CRL 1573)-expressing α3/β4 neuronal nAChRs (cell line designation: KXα3β4R_2 cells) were prepared as described previously (Xiao et al., 1998). Cells were plated in tissue culture medium (Gibco-BRL, Gaithersburg, MD) containing bovine serum and antibiotics. ACh^-, nicotine, and *d*-tubocuraine (*d*-tc) were obtained from Sigma Chemical Company (St. Louis, MO). Mecamylamine and epibatidine were purchased from Research Biochemicals (Natick, MA). A similar stable transfection of the rat α3/β4 receptor in HEK 293 cell line has been reported previously (Stetzer et al., 1996).

Cell Transfection and Culture. HEK 293 cells were maintained at 37°C with 5% CO_2 in the incubator. Growth medium for HEK 293 cells was minimum essential medium supplemented with 10% fetal bovine serum, 100 U/ml penicillin, 100 μg/ml streptomycin. Stably transfected cell lines were raised in selective growth medium containing 0.7 mg/ml of Geneticin (G418). Transfection was conducted by the calcium phosphate method (Chen and Okayama, 1987). Briefly, exponentially growing HEK 293 cells were plated in 100-mm dishes containing 10 ml of the growth medium 24 h before transfection. For transfection 1.0 ml of solution containing 10 μg of linearized DNA, 125 mM $CaCl_2$, 25 mM HEPES, 140 mM KCl, 6 mM glucose, 0.75 mM Na_2HPO_4 (pH 7.05) was added to the cell-containing dish in drop-wise fashion. The cells were incubated with the transfection mixture for 16 h in the incubator and then were grown in fresh growth medium for 24 h. They were collected and plated at a range of densities. The selection process was continued for 3 to 4 weeks. G418-resistant clones were picked up by cloning cylinders and have been maintained in continuous culture for about 1 year.

Electrophysiological Recording. Functional expression of nicotinic receptors was evaluated in the whole-cell configuration of the patch clamp technique using a DAGAN 8900 amplifier (Dagan Corp., Minneapolis, MN). The patch electrodes, pulled from borosilicate glass capillaries, had a resistance of 3 to 5 MΩ when filled with the internal solution containing (in mM): CsCl, 110; tetraethylammonium chloride, 20; NaCl, 0 to 20; MgATP, 5; EGTA, 14; HEPES, 20 and titrated to pH 7.2 with CsOH. About 90% of the electrode resistance was compensated electronically, so that effective series resistance in the cell-attached configuration was always less than 1 MΩ. Stably transfected HEK cells were studied 2 to 4 days after plating the cells on coverslips. Generation of voltage-clamp protocols and acquisition of data were carried out using pCLAMP software (Axon Instruments, Inc., Burlingame, CA). Sampling frequency was 0.5 to 2.0 kHz and current signals were filtered at 10 kHz before digitization and storage. All experiments were performed at room temperature (23–25°C). Currents were normalized relative to the membrane capacitance (10–30 pF) and then calculated as the mean ± S.E.M. for the number of cells examined (*n*).

Perfusion System. Cells plated on plastic coverslips (15 mm round thermanox, Nunc, Inc., Napierville, IL) were transferred to an experimental chamber mounted on the stage of an inverted microscope (Diaphot, Nikon, Nagano, Japan) and were bathed in a solution containing (in mM): NaCl, 137; $CaCl_2$, 2; HEPES, 10; glucose, 10; $MgCl_2$, 1 (pH 7.4 with NaOH). The experimental chamber was constantly perfused at a rate of about 1 ml/min with the control bathing solution. The amplitude and time course of the nicotinic current was highly dependent on the speed of application of nicotine. A reduction in flow rate significantly slowed the activation, decreased the amplitude, and slowed the desensitization of the nicotinic current (Callewaert et al., 1991). We therefore used servo-controlled miniature solenoid valves for rapid switching between control and test solutions (Cleemann and Morad, 1991). The effective switching time was determined in rat ventricular cells by measuring the peak Na^+ currents at various times after triggering a change in $[Na^+]_o$ or by measuring the holding current at the tip of an open patch pipette subjected to a solution of low Cl^- (Davies et al., 1988). Under optimal conditions, such changes in solution had a delay of 6 to 8 ms (corresponding mainly to the pull and release of the solenoid valves and replacement of fluid in the common outlet of the perfusion manifold) followed by a transition period where the measured current changed with a time constant of 5 to 10 ms. In repeated applications the delay was fairly reproducible, but it did show some variation in different experiments with different hydrostatic pressures and perfusion manifolds. The transition time was typically about 20 ms.

Confocal Microscopy. Nicotine-induced Ca^{2+} signals in single voltage-clamped HEK cells were measured by adding 1 mM of the fluorescent Ca^{2+} indicator dye fluo-3 to the dialyzing pipette solution and scanning the cell at a rate of 30 frames per second with a confocal microscope (Odyssey XL, Noran Inc., Madison, WI; microscope: Zeiss, Axiovert 135, 40× Zeiss 440052 c-apochromat objective, NA. 1.2). At this rate, the microscope collects full two-dimensional frames of 640 × 480 pixels on a 0.207 μm grid by collecting data at 10 MHz and sweeping the rapidly scanned direction with an acousto-optical deflector at 17 kHz. Detected fluorescent light passes through a variable slit extending in the rapidly scanned direction so that the instrument is confocal only in the slowly scanned direction. Ca^{2+} signals were measured as the change in fluorescence intensity over the entire cell, or they were normalized relative to the fluorescence intensity before application of nicotine (ΔF/F). Cells examined with confocal microscopy were cultured on 25-mm glass coverslips and subjected to reduced flow rates.

Results

Agonist-Induced Current. Stably transfected HEK 293 cells expressing α3/β4 nAChR generated rapidly activating inward current at −60 mV holding potentials when exposed

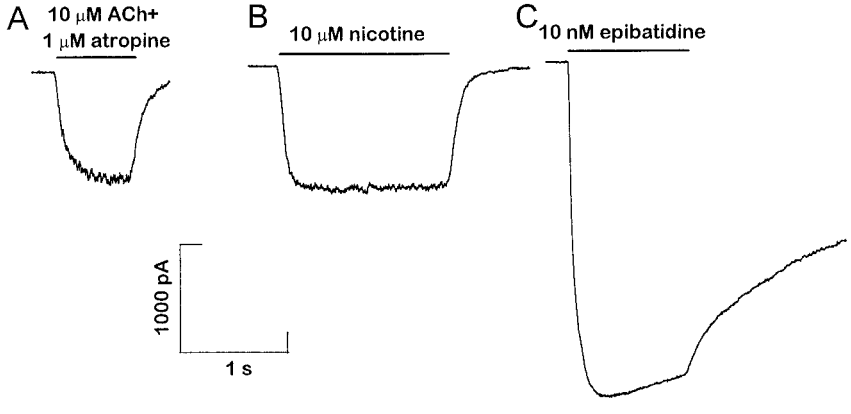

Fig. 1. Activation of currents through the α3/β4 receptor channel by different agonists. Currents were recorded at a constant holding potential of −60 mV with 30 s between each drug exposure. The traces are typical recordings from different cells. Notice that epibatidine is effective in a very low (nM) concentration (C).

to small concentrations of nACh receptor agonists. Figure 1 compares representative traces of current activated by application of 10 μM ACh (A), 10 μM nicotine (B), and 10 nM epibatidine (C). One micromolar concentrations of atropine were used to block any endogenous muscarinic receptors when ACh was used as an agonist. Because the time courses of activation and deactivation of the current on application and withdrawal of nicotinic agonists (Fig. 1) are significantly slower than the step change in agonist concentration (~20 ms; see Fig. 1B of Davies et al., 1988; Tang et al., 1989), it is possible that the time courses of rise and fall of the current reflect the binding or gating kinetics of the nAChR channel. Comparison of activation and deactivation of the current shows clearly that epibatidine-evoked currents decayed significantly slower on removal of the drug than those induced by acetylcholine, nicotine, and cytisine (Figs. 1 and 2, A and B), consistent with the higher binding affinity of the drug to the receptor (Xiao et al., 1998). Comparison of the peak currents generated by epibatidine and nicotine at −60 mV holding potentials showed that 10 nM epibatidine generated currents (88.3 ± 24.8 S.E.M. pA/pF, $n = 5$) equivalent to those activated by 200 μM ACh (93.0 ± 34.5 pA/pF, $n = 4$).

Dose-Response Relation. Figure 2 compares the dose dependence and kinetics of activation of $\alpha3/\beta4$ nAChR to rapid application of various concentrations of nicotine and cytisine. The dose-response (D) was measured by exposing each cell to at least three concentrations of either nicotine or cytisine. Nicotine and cytisine at concentrations of ~1 μM failed to activate a detectable current in $\alpha3/\beta4$-expressing cells. At higher concentrations (10–1000 μM) nicotine and cytisine evoked a rapidly activating inward current that varied in its magnitude and gating kinetics with concentration. The peak amplitude of nicotine- and cytisine-activated currents at −80 mV, when plotted as a function of agonist concentrations, showed that nicotine and cytisine at concentrations of 100 to 200 μM generally produced their maximal responses. The dose-response relationships were normalized and fitted with the empirical Hill equation $y = 1/(1+((EC_{50}/[\text{agonist}])^n))$ yielding a cooperativity factor (n), which was close to 2 for both agonists (nicotine: 1.96 ± 0.30; cytisine: 2.05 ± 0.17). The data indicate an EC_{50} of 22 ± 2 μM for nicotine and 64 ± 7 μM for cytisine. The magnitude of the fully activated current (corresponding to unity in Fig. 2D) was 121 ± 16 pA/pF ($n = 14$) in the group of cells activated by nicotine and 182 ± 20 pA/pF ($n = 11$) in the cells activated by cytisine, suggesting about equal efficacy for the two compounds.

The differential potency was tested by measuring the responses to 50 μM of both compounds in each of eight cells (Fig. 2, A-C). The results showed that the peak current activated by nicotine was about twice as large as that activated by cytisine. Consulting the dose-response curves (Fig. 2D), this is consistent with the notion of equal efficacy. Notice, however, that the rate of desensitization was consistently larger for nicotine than for cytisine, so that the currents after 500 ms of drug exposure were almost identical (Fig. 2C). This

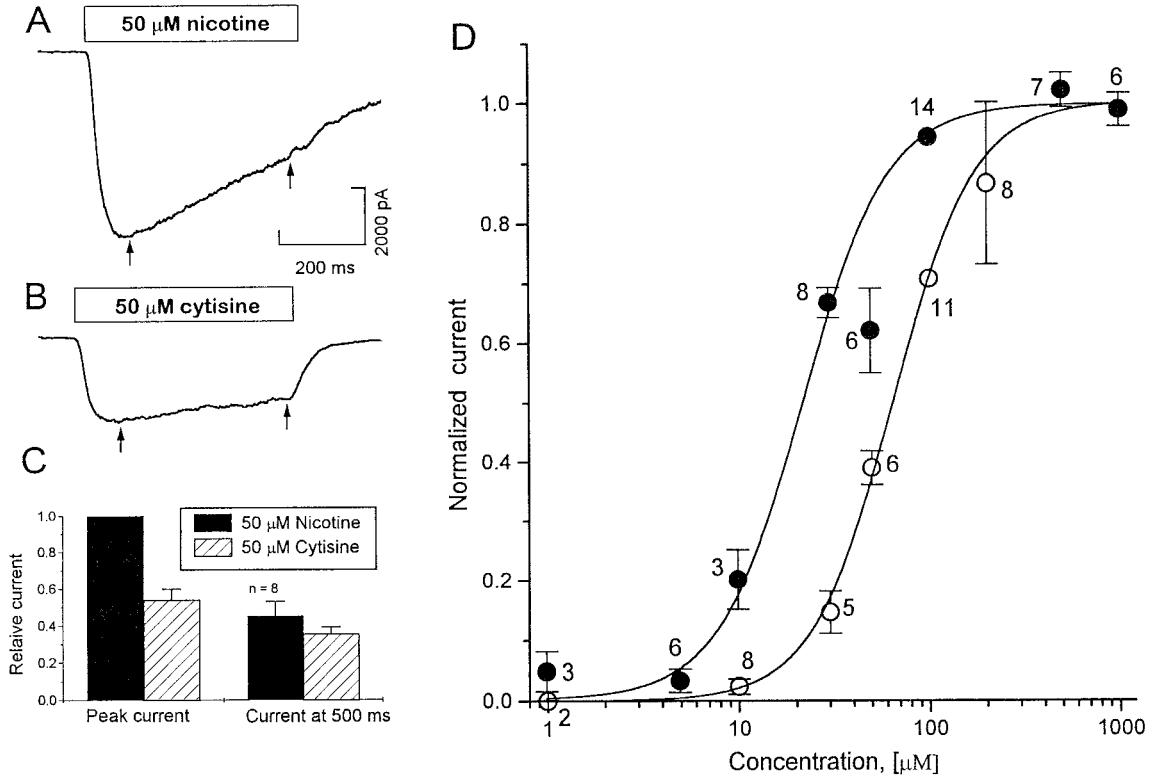

Fig. 2. Comparison of nicotinic currents activated by nicotine and cytisine. The sample records show typical currents activated at −80 mV in the same cell by 50 μM nicotine (A) or cytisine (B). C, average responses in eight such experiments where the peak and final (500 ms) currents (arrows in A and B) were normalized relative to the peak nicotine-induced current. D, dose-response curves for the peak currents induced by nicotine (●) and cytisine (○) at −80 mV. Before curve fitting, the currents induced by the two compounds were normalized relative to the current induced by 100 μM. After curve fitting with least-squares determination of EC_{50}, the data were normalized again to give a maximum response of one. Each symbol is labeled with a number indicating the number of cells tested and a vertical error bar indicating the S.E.M. The continuous curves represent a fit to the Hill equation with a cooperativity factor close to 2 (see text).

suggests that the relative potency and efficacy of nicotine and cytisine may depend on the speed of drug application and the timing of current or flux measurements.

Voltage Dependence of Agonist-Induced Current. Figure 3 compares the voltage dependence of three nAChR agonists. Comparison of superimposed tracings of the current activated with different agonist concentrations and test potentials shows that: 1) agonist-activated currents decay little at low concentrations and moderate holding potentials (~−40 mV) during a 1.5-s drug exposure period; 2) at higher concentrations, the current decays more rapidly after its activation; 3) little or no current is activated at 0 to +40 mV even when $[Na^+]_i$ was increased from 0 to 20 mM (data not shown); 4) the deactivation times increase at high agonist concentrations; and 5) the voltage dependence of the agonist-induced current displayed prominent inward rectification (Fig. 3, A-C, a characteristic of the whole-cell neuronal nAChR current measured in sympathetic neurons, Mathie et al., 1990; adrenal chromaffin cells, Callewaert et al., 1991; Nooney et al., 1992; and cultured hippocampal neurons, Bonfante-Cabarcas et al., 1996; or in HEK cells transiently transfected with α3/β4 nAChR**,** Wong et al., 1995).

Significant outward current was activated by nicotine or cytisine at potentials positive to +80 mV especially when using 200 to 1000 μM agonist concentrations (Fig. 3B). The voltage dependence of the epibatidine- and cytisine-induced current was similar to that of nicotine (Fig. 3A), i.e., large inward currents were measured at potentials negative to 0 mV with little or no current activated between 0 and 40 mV (Fig. 3, B and C). The most obvious difference between the epibatidine and nicotine or cytisine, in addition to the range of effective concentrations, was the off-rate of epibatidine current upon removal of the drug. Often at higher concentrations of epibatidine (1 μM), the activated current was significantly smaller than those generated by 100 nM epibatidine.

Intracellular magnesium has been proposed to regulate the rectification of the nicotinic current (Mathie et al., 1990; Albuquerque et al., 1997; Forster and Bertrand, 1995; Bonfante-Cabarcas et al., 1996). We also examined the effect of $[Mg^{2+}]_i$ on the voltage dependence of the nicotine-activated current, but found no significant change in the rectification or the voltage dependence of the current even when cells were dialyzed for 10 to 15 min with Mg^{2+}-free intracellular solutions containing 2 mM of the chelator EDTA (data not shown). Similarly, removal of extracellular Mg^{2+} had no measurable effects on the magnitude or the inward rectifying properties of the current. A similar insensitivity to Mg^{2+} was reported in α4/β2-expressing HEK cells (Buisson et al., 1996).

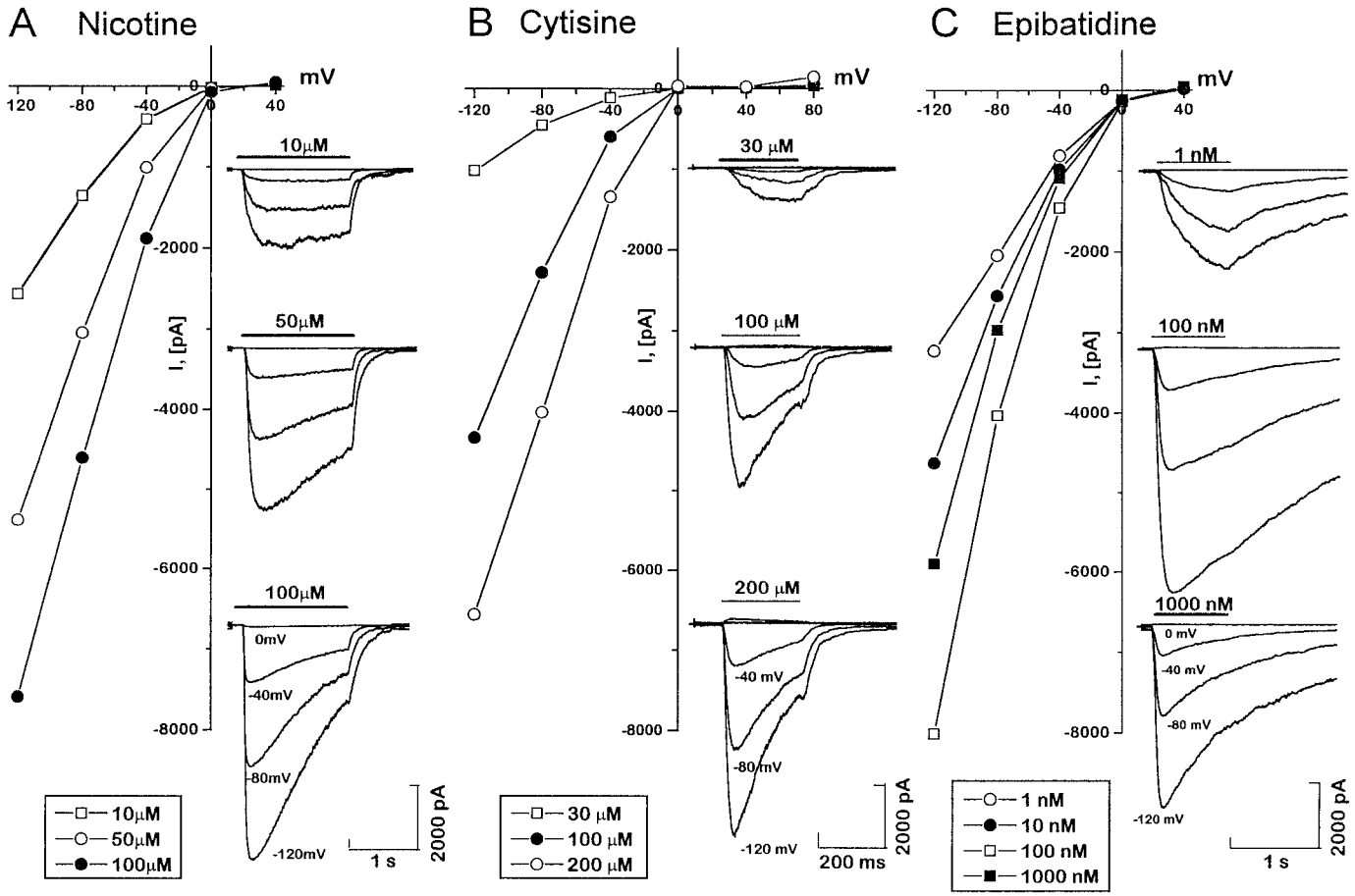

Fig. 3. Voltage dependence and time course of currents evoked by different concentrations of nicotine (A), cytisine (B), and epibatidine (C). Each panel is based on results from a single representative cell and shows current voltage relations of the maximal currents produced by the different drug concentrations. The box at the bottom of each panel indicates the drug concentration corresponding to each symbol. Notice that 1000 nM epibatidine (■, C) gives less current than 100 nM (□, C). Each of the three insets in each panel corresponds to a specific drug concentration and shows the current traces recorded at different potentials, as labeled.

Decay of Agonist-Activated Current. Nicotine-activated current decayed significantly in the presence of the drug, resulting in part from desensitization of the $\alpha 3/\beta 4$ receptor. Time constants of the decay of the current in the presence of nicotine typically ranged between 1.0 and 10.0 s, depending on the agonist concentration (Fig. 4A and B). After activation of the receptor by 30 μM, 100 μM, and 1 mM nicotine, the time constant of the decay of the current at -80 mV was found to be respectively 11 ± 6 ($n = 3$), 1.4 ± 0.3 ($n = 5$), and 2.0 ± 0.4 ($n = 4$) s (○, Fig. 4B). The rate constant of decay of the current was mostly independent of membrane potential (□, -120 mV; ○, -80 mV; △, -40 mV), but increased with increasing concentration (Fig. 4B).

At high nicotine concentrations, the decay kinetics of current may also reflect, in part, the block of the open channel by the agonist (Sine and Steinbach, 1984). Consistent with this idea, the rapid removal of 1 mM nicotine or cytisine were often accompanied by the activation of a "rebound" current, which may represent the rapid unblock of the channel by the agonist (Fig. 4A, top right; see also Fig. 7A). The rebound current was most prominent at voltages negative to -60 mV, was absent at voltages between -40 to $+80$ mV, was highly concentration-dependent, and appeared to be somewhat enhanced at higher concentrations of Ca^{2+} (Fig. 7A). A detailed analysis of the rebound current in muscle end-plate acetylcholine receptor has been recently reported by Maconochie and Steinbach (1998) using 1.0 to 10 mM ACh.

In some cells we observed a 10-fold faster rate of desensi-

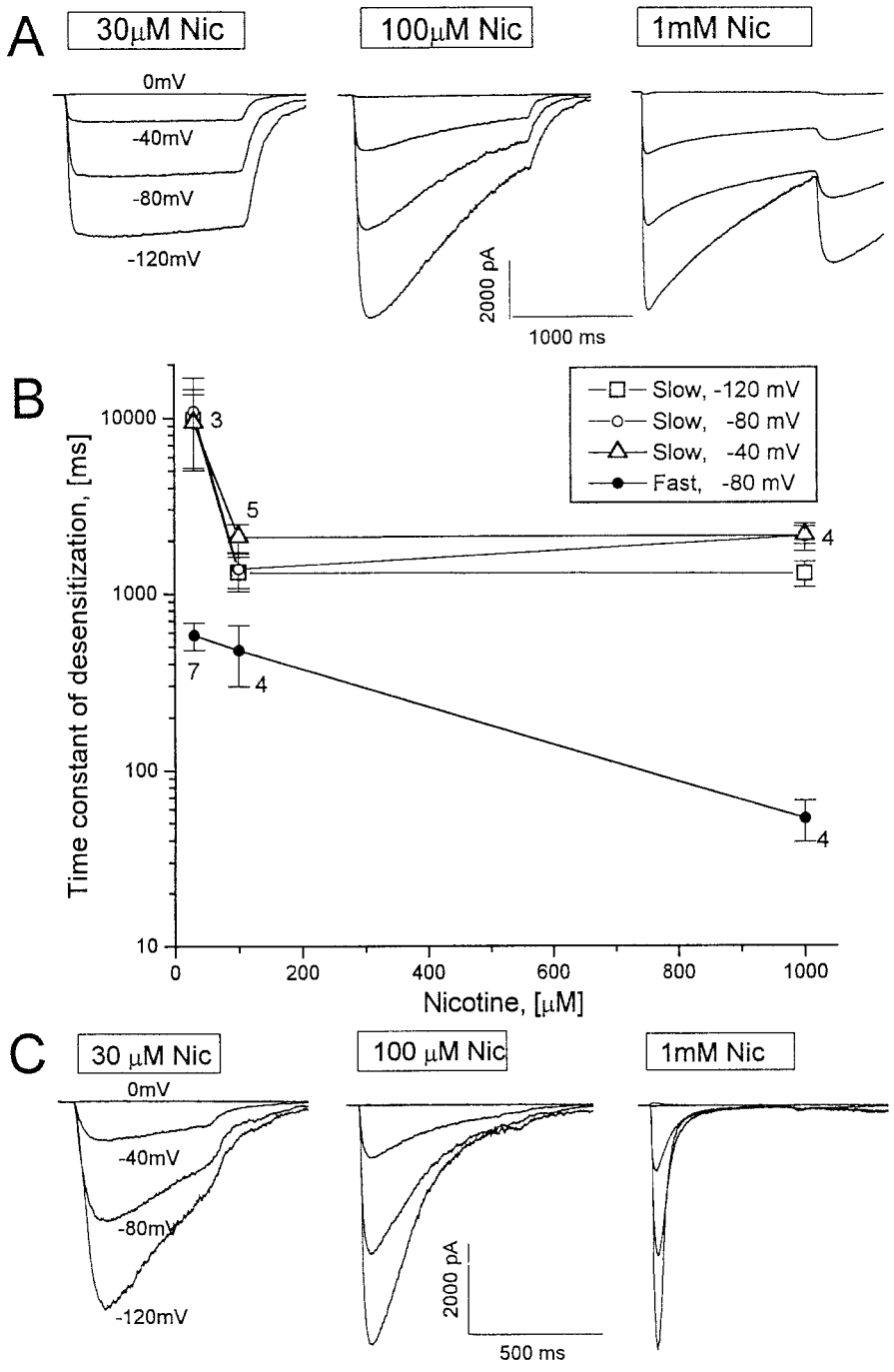

Fig. 4. Desensitization of the nicotine-induced current. The original records show typical currents evoked at different potentials (-120 mV, -80 mV, -40 mV, and 0 mV) by different concentrations of nicotine (30 μM, 100 μM, and 1 mM) in different cells with slow (A) or fast (C) desensitization. B, concentration dependence of the time constant of desensitization in cells with slowly decaying currents measured at -120 mV (□), -80 mV (○), and -40 mV (△), and in cells with rapidly decaying currents measured at -80 mV (●). Each symbol is labeled with number of experiments and a vertical error bar.

tization (Fig. 4C), which was also accelerated by increasing nicotine concentrations (● Fig. 4B). The cells on a given day of experimentation would all have either slow or fast desensitization. During an experiment lasting 5 to 20 min the time constant of desensitization would often decrease by a factor of 2, but not enough to alter a slowly desensitizing cell to a fast one.

Nicotine-Activated Current Was Blocked by Mecamylamine and *d*-tc. To further characterize the properties of the nicotine-induced current in α3/β4-expressing cells, we examined the kinetics, voltage, and concentration dependence of two well known nAChR blockers. To determine the relative speed of the antagonist action vis-à-vis the agonist-activated current, nicotine and the antagonist were coapplied to the cell. Rapid application of mecamylamine (1 μM) simultaneous with 10 μM nicotine suppressed the nicotine-induced current by ≅80% (n = 4; Fig. 5A and C). The suppressive effect of the drug was voltage-dependent such that at −120 mV, mecamylamine blocked the current by ~80% versus ~60% at −80 mV (Fig. 5B). Mecamylamine also significantly enhanced the decay kinetics of the nicotine-activated current, consistent with the open channel-blocking property of the drug (Fig. 5A). Nicotine-activated current recovered rapidly upon washout of the blocker. Thus, mecamylamine appears to access the channel pore in a voltage- and time-dependent manner. The kinetics of the block at the 1 μM concentration were sufficiently fast as to prevent most of the nicotine-activated current when the agonist and antagonist were coapplied.

Similarly, *d*-tc (50 μM) when coapplied with 30 μM nicotine blocked the current rapidly (Fig. 6). Concentrations of *d*-tc smaller than 10 μM, when coapplied with nicotine, had little or no effect on the current activated by nicotine (n = 3, data not shown). The onset of *d*-tc block, similar to mecamylamine, was fast and consistent with channel-blocking properties of these drugs (Fig. 6A).

Calcium Permeation and Block of Rat α3/β4 nAChR. Reliable measurements of reversal potential are required to assess directly the ionic selectivity of agonist-induced current. Because little or no outward current could be measured on activation of the nicotinic receptor between 0 and +40 mV, the measurements of reversal potentials were less reliable. Thus, we attempted to evaluate the permeation of Ca^{2+} based on the larger current measured at very negative and positive potentials.

Figure 7A shows how the current through the α3/β4 nAChR was modified when the external Ca^{2+} concentrations were increased from 2.0 to 10 mM during application of 50 μM nicotine. At −120 mV and −80 mV the higher $[Ca^{2+}]_o$ suppressed the current and the washout of the drug was accompanied by a noticeable rebound current, as if the blocking effect of Ca^{2+} washed out before the deactivation of the

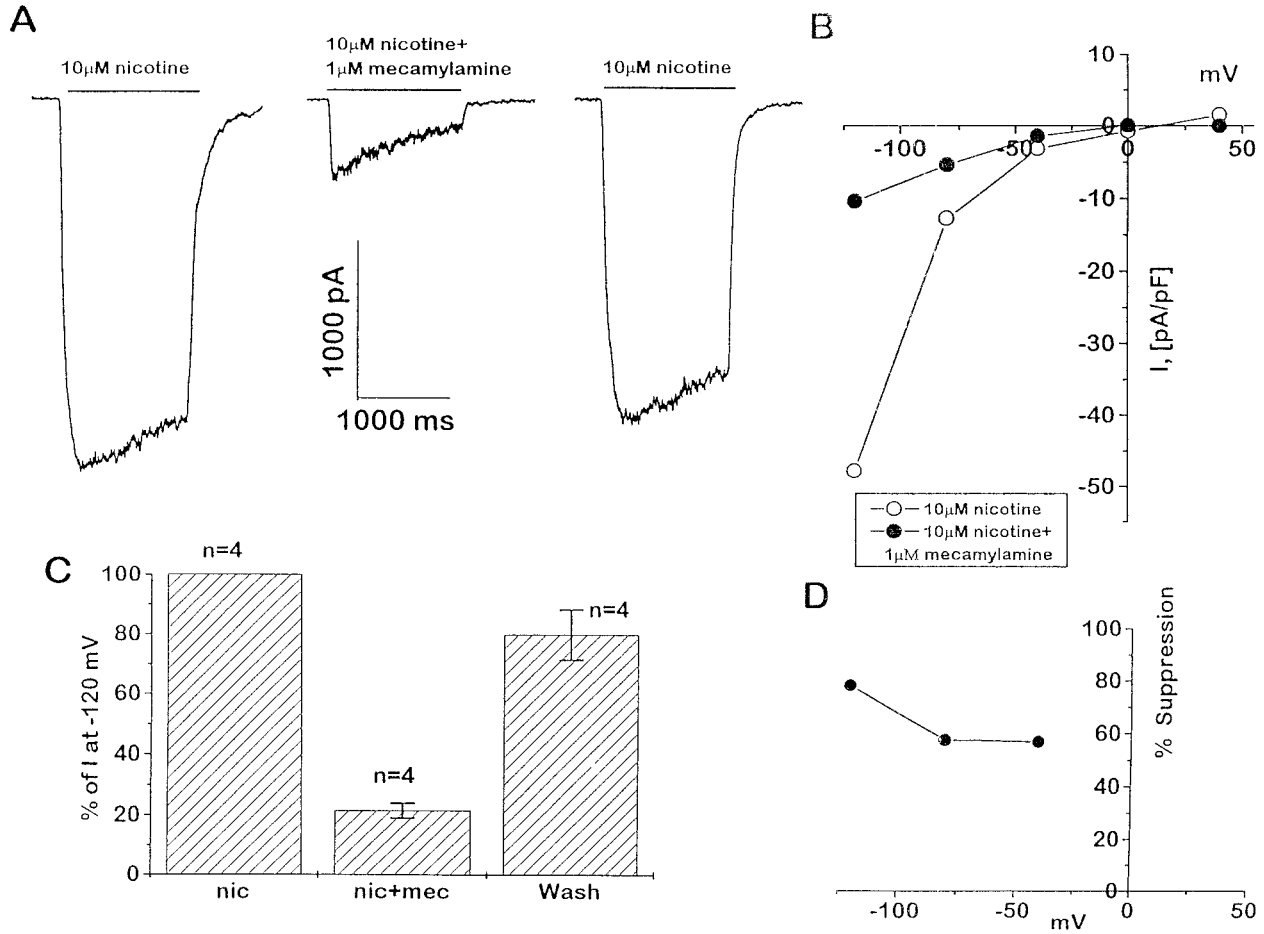

Fig. 5. Block of nicotine-induced current by mecamylamine. A, reversible suppression of nicotine-induced current at −120 mV by 1 μM mecamylamine. B, voltage dependence of nicotine-induced current in the absence (○) and presence (●) of mecamylamine. C, average effect of mecamylamine effect (A) in four cells (at −120 mV). D, voltage dependence of mecamylamine block.

channel. In addition, the current activated by 50 μM nicotine, at -80 mV, was slightly suppressed when $[Ca^{2+}]_o$ was reduced to 0.2 mM (○, Fig. 7B). This trend became significant in completely Ca^{2+}-free solution over a wide range of nicotine concentrations (20 (■), 200 (●) μM nicotine). Significant suppressions were also observed at 5 and 10 mM $[Ca^{2+}]_o$. Complete replacement of all the external NaCl with 90 mM $CaCl_2$, completely blocked the inward current through the receptors during the drug exposure period (Fig. 7B) and suppressed the outward current at +120 mV to 18 ± 11% ($n = 5$) of values measured with 2 mM $[Ca^{2+}]_o$. Thus, if Ca^{2+} in addition to its blocking effect were also to permeate the channel, it would most likely generate significant current at the moderate Ca^{2+} concentrations. Accordingly, at 10 mM Ca^{2+} (Fig. 7C), the nicotine-induced currents appeared to decrease at -120, -80, and +120 mV, increase at -40 mV and remain undetectable at 0 and +40 mV. These changes were significant when measured relative to the current recorded in control solution with 2 mM Ca^{2+}. The enhanced inward current at -40 mV suggest that Ca^{2+} may permeate through the nAChR channel and shift the reversal potential toward more negative potentials.

To determine more directly whether activation of nicotine-induced current results in rise of $[Ca^{2+}]_i$, we measured confocal images of Ca^{2+} in Fluo 3-dialyzed voltage clamped cells. Figure 8A shows simultaneous traces of nicotine-activated current and intracellular Ca^{2+} in response to rapid application of 100 μM nicotine recorded at indicated locations in the cell. Cytosolic Ca^{2+} appears to rise more rapidly at peripheral and flatter segments of the cell (Fig. 8B, open symbols; see also Fig. 9) than at the thicker midsection of the cell (Fig. 9B, closed symbols) even though the thicker segments seem to achieve higher "apparent" Ca^{2+} concentrations. Intracellular Ca^{2+} ($\Delta F/F$) rises continuously during the application of nicotine and decays slowly upon removal of nicotine. Comparison of total charge carried by the nicotinic channel in five different cells (represented by different symbols in Fig. 8C) and change in fluorescence ($\Delta F/F$) showed direct correspondence of current and $\Delta F/F$ (Fig. 8C), suggesting that the rise in Ca^{2+} is directly correlated to the ionic charge transported by the $\alpha 3/\beta 4$ receptor. Mecamylamine strongly suppressed the nicotine-activated current and simultaneously inhibited the rise in $[Ca^{2+}]_i$ (Fig. 8C, open symbols), suggesting that the nicotinic channel was responsible for the rise in Ca^{2+}.

The experiment illustrated in Fig. 9 was performed to test the possibility that the influx and intracellular accumulation of Na^+ might mediate the rise in cytosolic Ca^{2+} via transport of Ca^{2+} on the Na^+-Ca^{2+} exchanger. Such a mechanism might be accentuated in flatter and narrower parts of the cell where Na^+ as well as Ca^{2+} could readily build up as a result of large agonist-activated current. We therefore compared the Ca^{2+} signals measured at -80-mV holding potentials, when K^+ was substituted as extracellular charge carrier for Na^+. In a set of three experiments, we found that nicotine-

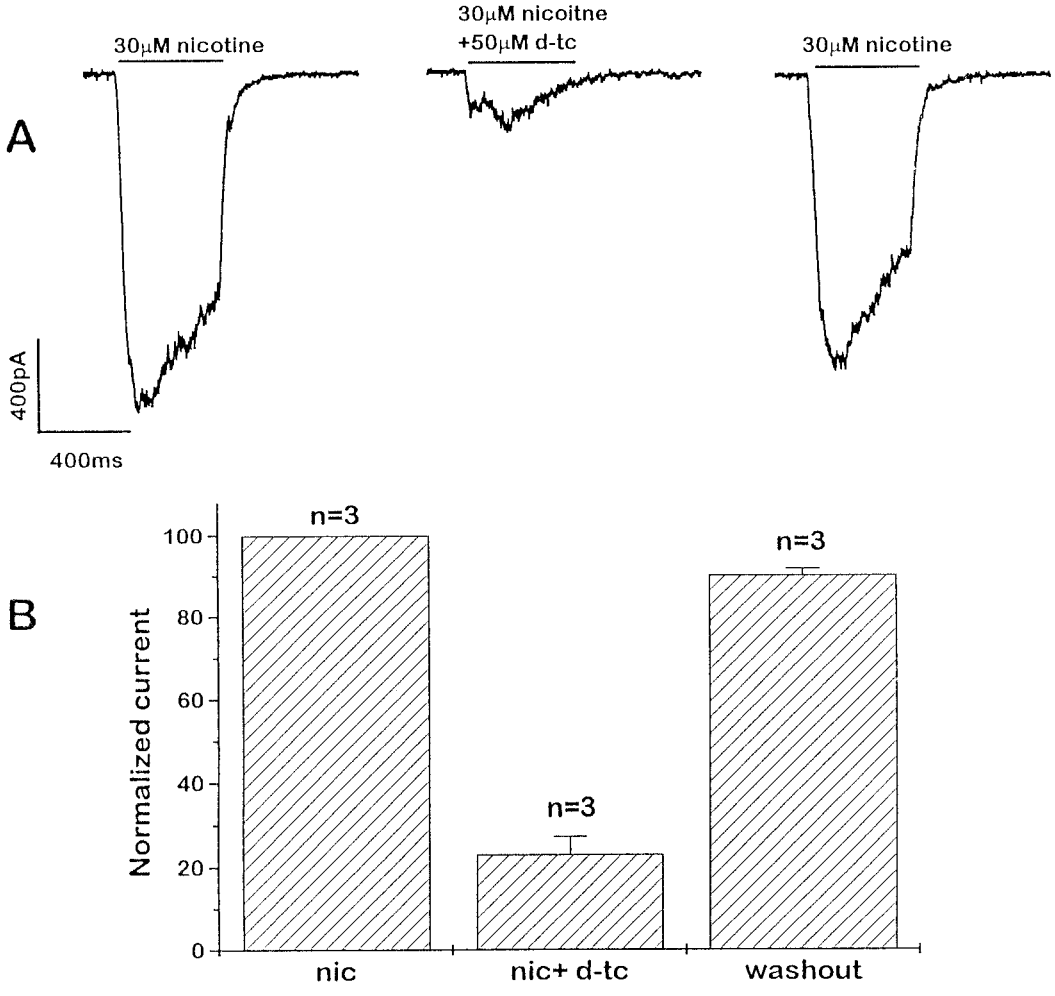

Fig. 6. Block of nicotine-induced current by *d*-tc. A, reversible suppression of nicotine-induced current by 50 μM *d*-tc. B, average effect *d*-tc effect (A) in three cells.

activated currents and the rise in cytosolic Ca^{2+} were similar whether Na^+ (Control) or K^+ (KCl) was the charge carrier through the channel (Fig. 9). The inset frames of Fig. 9 show that the ratiometric Ca^{2+} signals ($\Delta F/F$) increase in strength toward the distal ends of the cellular protrusions more rapidly than the center of the cell and confirm that K^+ substitution alters neither the magnitude nor the cellular distribution of the Ca^{2+} signals. Because K^+ is known not to substitute for Na^+ on the Na^+-Ca^{2+} exchanger, this finding strongly suggests that the Ca^{2+} signals are not produced secondary to influx of Na^+, but are directly related to the permeation of Ca^{2+} via the nAChR channel.

Discussion

In response to application of nicotinic agonists (ACh, nicotine, cytisine, and epibatidine), HEK cells stably transfected with rat α3/β4 nAChR generate a large rapidly activating and slowly decaying current. This current displayed inwardly rectifying properties (generating little or no current between 0 and +40 mV, Fig. 3) and was rapidly and reversibly blocked by mecamylamine and *d*-tc (Figs. 5 and 6). The nicotine-activated channel, at physiological Ca^{2+} concentrations, appears to transport sufficient Ca^{2+} as to induce significant rise in cytosolic Ca^{2+} concentrations (Figs. 8 and 9). At higher concentrations, Ca^{2+} appears to suppress the Na^+ current through the receptor, consistent with Ca^{2+} serving as a permanent blocker, but the complete block of the channel on isoosmolar replacement of Na^+ by Ca^{2+} may suggest an additional regulatory role for extracellular Ca^{2+}.

Dose-Response of Nicotine and Cytisine. Nicotine and cytisine appeared to activate the α3/β4 recombinant receptor with EC_{50} values of about 22 and 64 μM, respectively, and with a cooperativity factor of ~2.0 for both agonists. Hill coefficients ranging between 1.5 and 2.0 have been reported previously for both the recombinant and wild types of nAChR (Lindstrom, 1995; Wong et al., 1995). Significantly lower Hill coefficients of 0.6 and 1.4 were recently reported for the human α3/β4 recombinant receptor stably expressed in HEK cells (Stauderman et al., 1998). However, in those experi-

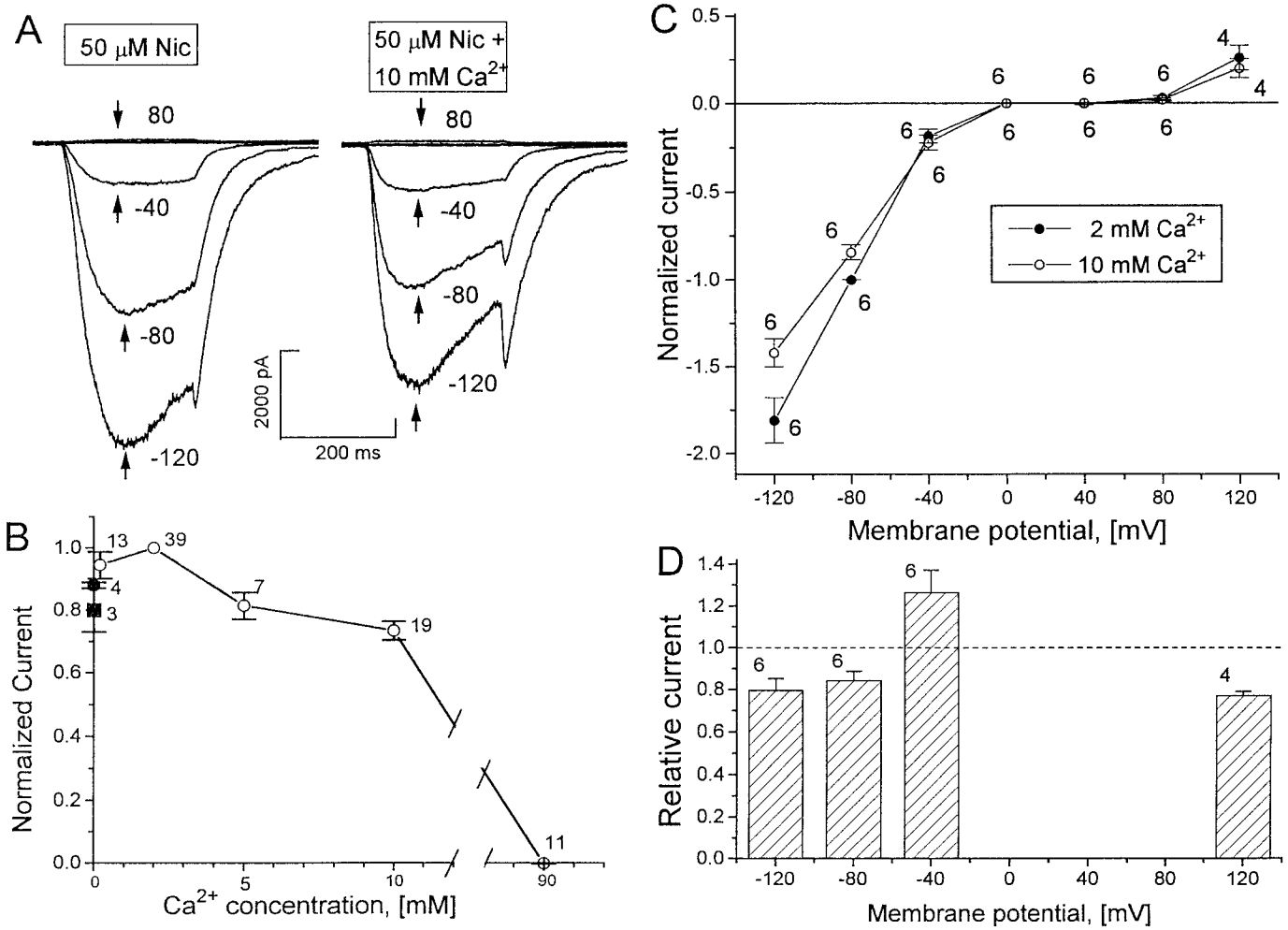

Fig. 7. Modulation of the nicotine-induced current by extracellular calcium. A, sample records showing the currents induced by 50 μM nicotine when added to the standard Tyrode's solution with 2 mM Ca^{2+} (left) and when administered together with 10 mM Ca^{2+}. The traces are labeled with the membrane potential in mV. B, effect of extracellular Ca^{2+} on the current induced by 20 (■), 50 (○), or 200 (●) μM nicotine. Currents were measured as the peak value at −80 mV relative to the average value of bracketing recordings at 2 mM $[Ca^{2+}]_o$. The number next to each data point indicates the number of cells examined. C, average effect of 10 mM Ca^{2+} on the voltage relations of the currents induced by 50 μM nicotine. The currents in each experiment were measured as the average over a 60-ms interval (from 60–120 ms after application of nicotine) and was normalized relative to the current measured at −80 mV in control solution with 2 mM Ca^{2+}. D, modulating effect of 10 mM Ca^{2+} on the current evoked by nicotine at different potentials.

ments, the coefficients were derived from measurements of intracellular Ca^{2+} in large populations of cells in response to slow application of nicotinic receptor agonists and could reflect both desensitization of the receptor and indirect functional coupling between activation of nicotinic receptor and rise in $[Ca^{2+}]_i$. Our electrophysiological measurements, based on rapid application of agonists, on the other hand, appear to fit a Hill coefficient close to 2.0 for both cytisine and nicotine (Fig. 2) as found also with human $\alpha3/\beta4$ expressed in oocytes (Chavez-Noriega et al., 1997). Cytisine is generally reported to be at least as potent as nicotine in activating the $\alpha3/\beta4$ receptor to generate inward current in oocytes (Chavez-Noriega et al., 1997; Gerzanich et al., 1998) or Ca^{2+} influx in HEK cells (Stauderman et al., 1998). In our experiments, we found a somewhat higher EC_{50} value for cytisine (Fig. 2D). However, this may be in part due to measuring the current shortly after the drug application and before the development of agonist-induced block or desensitization (Fig. 2, A-C). Because such rapid measurements are not possible in whole oocytes or dense populations of eukaryotic cells where average activation times of the receptor are significantly slower (>5 s), the previously reported dose-response relations may reflect the steady-state component of the agonist-activated current.

Decay of Nicotine-Activated Current. The rate of decay of nicotine-induced current in the presence of nicotine was strongly concentration-dependent, such that at low concentrations of agonists (10–30 μM) time constants in excess of 10 s were required for full decay of the current, whereas at 100 to 1000 μM drug concentrations the current decayed within 1 to 2 s (Fig. 4).

Although it is tempting to attribute the decay of the current entirely to the desensitization of the receptor, the decay of current in the presence of the agonist may also reflect, in part, agonist-induced block of the channel. This might be particularly the case at higher concentrations of agonists, as demonstrated for the muscle endplate nicotinic receptors (Sine and Steinbach, 1984; Maconochie and Steinbach, 1998). The bell-shaped dose-response relation was also seen in the $\alpha3/\beta4$-expressing HEK cells in our laboratory using Rb^+ efflux to measure channel function (Xiao et al., 1998). That agonist may serve as a channel blocker at high concentra-

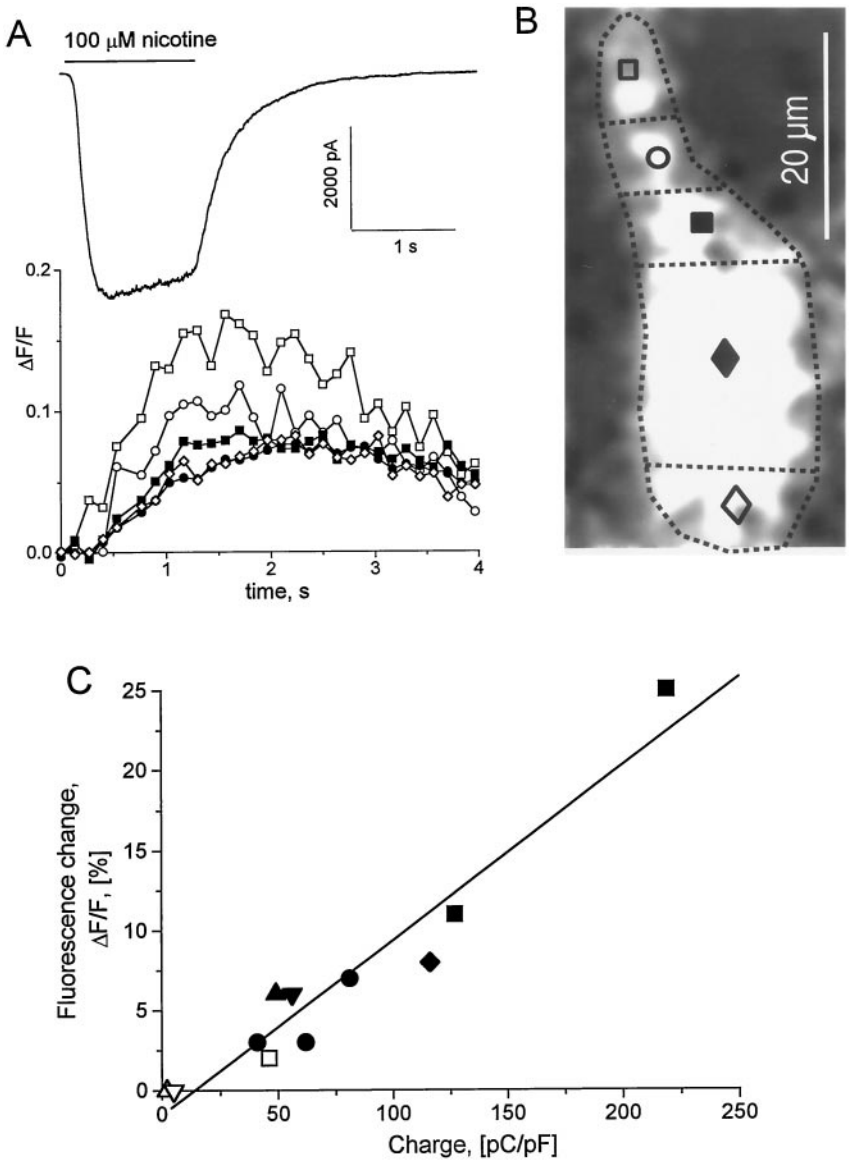

Fig. 8. Nicotine-induced Ca^{2+} signals. A, time course of the current evoked by exposure to 100 μM nicotine (top) and the normalized change in fluorescence intensity ($\Delta F/F$) measured in different regions of the cell. Each data point was measured as the average during four frames and is labeled with a symbol corresponding to a region in (B). The fluorescence image in (B) was measured differentially (ΔF) as the rise in fluorescence at the peak of the response (1–2 s) relative to signal at rest (0–0.5 s). C, compares the fluorescence signal ($\Delta F/F$) to the integral of the nicotine-induced current (charge) in five cells indicated with symbols of different shapes. Open symbols represent measurements performed in three cells in the presence of 5 μM mecamylamine. The holding potential in different cells ranged between −60 and −100 mV.

tions is also consistent with significant acceleration in the decay kinetics of α3/β4-generated current (Fig. 3) and the enhancement of "rebound" current at negative potentials (Figs. 3B, 4A, and 7A). Our data are, therefore, consistent with the idea that at higher concentrations and negative potentials ACh, nicotine, and cytisine may gain access to the channel permeation sites and serve as open channel blockers (see scheme proposed by Colquhoun et al., 1987; Maconochie and Steinbach, 1998).

Comparing the kinetics of decay of nicotine-activated current in α3/β4-expressing HEK cells with those of primary cultures of adult rat chromaffin cells exposed to the same set of experimental conditions and techniques suggests significantly slower decay kinetics of ACh- or nicotine-activated current in recombinant versus the native receptor. The time constant of decay of nicotinic current in primary cultures of rat chromaffin cells was 324 ± 58 ms (n = 5) when activated with 30 μM and 128 ± 26 ms (n = 5) with 1 mM nicotine compared with 10.9 ± 5.9 s (n = 3) and 2.1 ± 0.3 s (n = 4), respectively, in transfected HEK cells expressing the α3/β4 recombinant receptor.

In some populations of cells, the rate of decay of the current was much faster, by as much as an order of magnitude (cf. Fig. 4, A and C), approaching the decay kinetics of the cur-

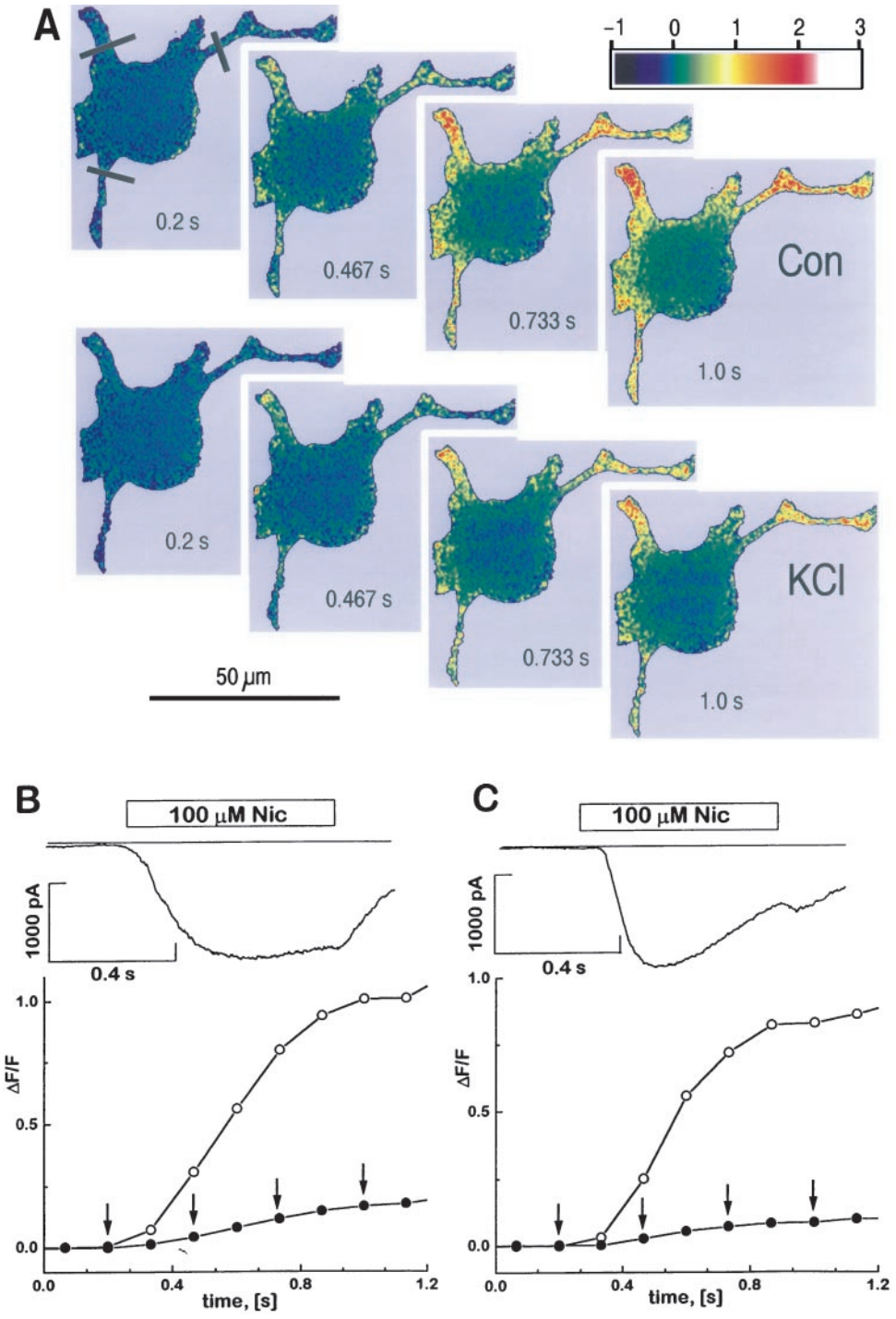

Fig. 9. Ca^{2+} signals evoked by permeation of Na^+ (B) or K^+ (C) through the nAChR channel. A, shows two sets of sample frames measured with confocal microscopy as nicotinic currents were activated with either Na^+ or K^+ as charge carrier. Each of the shown frames was obtained by averaging four frames recorded at 30 Hz and dividing by the average of 16 frames recorded before exposure to 100 μM nicotine. The graphs show the nicotinic currents and Ca^{2+} signals recorded in control solution with Na^+ as charge carrier (B) and after replacement of extracellular Na^+ with K^+ (C). (●) correspond to the average signal from cell body portions of the cell whereas (○) correspond to average fluorescence over the three major protrusions as defined by black lines in the sample frames. The Ca^{2+} signals (ΔF/F) in the graphs were obtained by averaging four frames for each point and integrating over the relevant areas of the cell before normalization. Arrows indicate the timing of the sample frames.

rent recorded in primary cultures of rat chromaffin cells (Callewaert et al., 1991). Such cell populations were relatively rare, and their occurrence could not be attributed to any known culture or experimental condition.

The kinetics of decay of $\alpha3/\beta4$ current reported here are significantly faster than those recently reported for this receptor expressed in *Xenopus* oocytes. At 50 μM nicotine concentrations, time constants of about 200 s were measured in oocytes (Fenster et al., 1997), compared with about 1.0 s in HEK cells (Fig. 4). Such differences may reflect the role of host cells in determining the regulatory properties of neuronal nicotinic receptors (Lester and Dani, 1995).

Ca^{2+} Permeability of $\alpha3/\beta4$ Receptor. Permeation of Ca^{2+} through the native and the recombinant nicotinic receptor has been the subject of considerable interest and investigation. From the shift in the reversal potential, on fractional increases of extracellular Ca^{2+}, a P_{Ca}/P_{Na} of 0.9 for $\alpha3/\beta4$ and 0.1 for the muscle $\alpha1/\beta1/\gamma/\delta$ expressed in oocyte have been estimated (Costa et al., 1994). Direct comparison of charge transported by the channel and the rise of intracellular Ca^{2+} measured in chromaffin cells and in oocytes expressing $\alpha3/\beta4$ suggest that approximately 2 to 4% of the total charge may be transported by Ca^{2+} at physiological Ca^{2+} concentrations (Vernino et al., 1992; Decker and Dani, 1990). Unexpectedly, however, Vernino et al. (1992) also found that a 10-fold increase in $[Ca^{2+}]_o$ also enhanced the outward current through the $\alpha3/\beta4$ receptor at positive (+30 mV) membrane potentials, where enhancement of inward Ca^{2+} current was expected (see also Amador and Dani, 1995). These findings support the idea that Ca^{2+} may both permeate and allosterically regulate the nAChR from an extracellular site (Lena and Changeux, 1993). Consistent with a possible regulatory role of Ca^{2+} on nAChR, Buisson et al. (1996) reported a 50% suppression of the current on a 10-fold increase of $[Ca^{2+}]_o$ in $\alpha4/\beta2$-transfected HEK cells. The decrease in the whole-cell current appears to be carried by suppression of the single channel conductance on elevation of $[Ca^{2+}]_o$ in both the native and recombinant receptors (Vernino et al., 1992; Mulle et al., 1992; Amador and Dani, 1995; Buisson et al., 1996).

Our electrophysiological data on $\alpha3/\beta4$-transfected HEK cells showed a bell shaped response for the magnitude of the current versus the extracellular Ca^{2+} concentration (Fig. 7B). The reduction of the current at low Ca^{2+} concentrations (Fig. 7B) may in part reflect a surface charge effect that would shift the current-voltage relations to the left when the divalent cation concentrations were lowered. The elevations of Ca^{2+} from 2 to 10 to 90 mM partially or completely (Fig. 7B) blocked the nicotine-activated current, consistent with the data in $\alpha4/\beta2$-expressing HEK cells (Bouisson et al., 1996). However, detailed examination of the current-voltage relations (Fig. 7C) showed that elevation of $[Ca^{2+}]_o$ increased the inward current at −40 mV. This finding is consistent with the measurements in oocytes where the currents are large enough to reveal the effects of Ca^{2+} at and near the reversal potential (Gerzanich et al., 1998). Our findings are in part consistent with the idea that Ca^{2+} permeates through the nAChR channel, but in the process briefly occludes the channel, thereby lowering its single channel conductance. However, such a mechanism would require that the blocking effect depend on the electrical potential driving Ca^{2+} into the channel, somewhat inconsistent with Fig. 7D where the degree of block appears to be equivalent at −120 mV and +120 mV.

Direct measurement of intracellular Ca^{2+} (Figs. 8 and 9) shows that the rise in intracellular Ca^{2+} was directly related to the magnitude of the charge transferred through the receptor (Fig. 8, a 10–30% rise of $\Delta F/F$ for currents ranging from 1.5–4 nA). Because these cells were dialyzed with 1 mM fluo-3 ($K_d \cong 300$ nM) and assuming resting Ca^{2+} activity of $\cong$100 nM, the predicted rise in $[Ca^{2+}]_i$ is about 33 to 100 μM, producing $P_{Ca}/P_{Na} \approx 1$, consistent with the P_{Ca}/P_{Na} values measured in native cells or $\alpha3/\beta4$ receptor expressed in oocytes (Costa et al., 1994; Vernino et al., 1992), but is not easily reconciled with the complete suppression of inward current after replacement of all Na^+ with Ca^{2+} (Fig. 7B). We also considered whether the rise in cytosolic Ca^{2+} occurs indirectly through a voltage-gated Ca^{2+} channel or via the Na^+-Ca^{2+} exchanger. The persistence of the Ca^{2+} signals at −80 mV and when Na^+ was replaced by K^+ as the charge carrier (Fig. 9), however, suggests that Ca^{2+} permeates directly through the nAChR channel. Thus, fairly small and difficult to detect Ca^{2+} currents through the $\alpha3/\beta4$ receptor may cause significant increases in cytosolic Ca^{2+} in transfected HEK cells (average cell volume and capacitance, 4 pl and 20 pF; Figs. 8 and 9). Although our Ca^{2+} imaging data are consistent with the findings of others on native and recombinant $\alpha3/\beta4$ receptor measured in neurons, oocytes, and eukaryotic cells, the suppressive effect of Ca^{2+} on the $\alpha3/\beta4$ receptor appears to be more consistent with that observed in HEK cells (Bouisson et al., 1996) rather than oocytes (Vernino et al., 1992). It is intriguing to speculate whether the regulation of Ca^{2+} permeability of nAChR may, in part, depend on endogenous presence of other Ca^{2+}-sensitive ion transporters or subunit assembly of the receptor in the host cells (Lewis et al., 1997; Cooper and Miller, 1997).

References

Albuquerque EX, Alkondon M, Pereira EFR, Castro NG, Schrattenholz A, Barbosa CTF, Bonfante-Cabarcas R, Aracava Y, Eisenberg HM and Maelicke A (1997) Properties of neuronal nicotinic acetylcholine receptors: Pharmacological characterization and modulation of synaptic function. *J Pharmacol Exp Ther* **280:**1117–1136.

Amador M and Dani JA (1995) Mechanism for modulation of nicotinic acetylcholine receptors that can influence synaptic transmission. *J Neurosci* **15:**4525–4532.

Anand R, Conroy WG, Schoepfer R, Whiting P and Lindstrom J (1991) Neuronal nicotinic acetylcholine receptors expressed in *Xenopus* oocytes have a pentameric quaternary structure. *J Biol Chem* **266:**11192–11198.

Bonfante-Cabarcas R, Swanson KL, Alkondon M and Albuquerque EX (1996) Diversity of nicotinic acetylcholine receptors in rat hippocampal neurons. IV. Regulation by external Ca^{2+} of α-bungarotoxin-sensitive receptor function and of rectification induced by internal Mg^{2+}. *J Pharmacol Exp Ther* **277:**432–444.

Boulter J, Connolly JG, Deneris ES, Goldman D, Heinemann S and Patrick J (1987) Functional expression of two neuronal nicotinic acetylcholine receptor from cDNA clones identifies a gene family. *Proc Natl Acad of Sci USA* **84:**7763–7767.

Buisson B, Gopalakrishnan M, Arneric SP, Sullivan JP and Bertrand D (1996) Human $\alpha4\beta2$ neuronal nicotinic acetylcholine receptor in HEK 293 cells: A patch-clamp study. *J Neurosci* **16:**7880–7891.

Callewaert G, Johnson RG and Morad M (1991) Regulation of the secretory response in bovine chromaffin cells. *Am J Physiol* **260:**C851–C860.

Chavez-Noriega L, Crona J, Washburn M, Urrutia A, Elliott K and Johnson C (1997) Pharmacological characterization of recombinant human neuronal nicotinic acetylcholine receptors h$\alpha2\beta2$, h$\alpha2\beta4$, h$\alpha3\beta2$, h$\alpha3\beta4$, h$\alpha4\beta2$, h$\alpha4\beta4$, h$\alpha7$ expressed in *Xenopus Oocytes. J Pharmacol Exp Ther* **280:**346–356.

Chen C and Okayama H (1987) High-efficiency transformation of mammalian cells by plasmid DNA. *Mol Cell Biol* **7:**2745–2752.

Cleemann L and Morad M (1991) Analysis of role of Ca^{2+} channel in cardiac excitation contraction coupling: Evidence from simultaneous measurements of intracellular Ca^{2+} contraction and Ca^{2+} current. *J Physiol* **432:**283–312.

Colquhoun D, Ogden DC and Mathie A (1987) Nicotinic acetylcholine receptors of nerve and muscle: Functional aspects. *Trends Pharmacol Sci* **8:**465–472.

Connolly JG, Gibb AJ and Colquhoun D (1995) Heterogeneity of neuronal nicotinic acetylcholine receptors in thin slices of rat medial habenula. *J Physiol* **484:**87–105.

Cooper ST and Miller NS (1997) Host cell-specific folding and assembly of the neuronal nicotinic acetylcholine receptor $\alpha7$ subunit. *J Neurochem* **68:**2140–2151.

Costa CS, Patrick JW and Dani JA (1994) Improved technique for studying ion

channels expressed in *Xenopus* oocytes, including fast superfusion. *Biophys J* **67:**395–401.
Davies NW, Lux HD and Morad M (1988) Site and mechanism of activation of proton-induced sodium current in chick dorsal root ganglion neurones. *J Physiol* **400:**159–187.
Decker ER and Dani JA (1990) Calcium permeability of the nicotinic acetylcholine receptor: The single-channel calcium influx is significant. *J Neurosci* **10:**3413–3420.
Fenster CP, Rains MF, Noerager B, Quick MW and Lester RAJ (1997) Influence of subunit composition on desensitization of neuronal acetylcholine receptors at low concentrations of nicotine. *J Neurosci* **17:**5747–5759.
Forster I and Bertrand D (1995) Inward rectification of neuronal nicotinic acetylcholine receptors investigated by using the homomeric α7 receptor. *Proc R Soc Lond Ser B* **260:**139–148.
Gerzanich V, Wang F, Kuryatov A and Lindstrom J (1998) α5 Subunit alters desensitization, pharmacology, Ca^{2+} permeability and Ca^{2+} modulation of human neuronal α3 nicotinic receptors. *J Pharmacol Exp Ther* **286:**311–320.
Lena C and Changeux JP (1993) Allosteric modulation of nicotinic acetylcholine receptor. *Trends Neurol Sci* **16:**181–186.
Lester RAJ and Dani JA (1995) Acetylcholine receptor desensitization induced by nicotine in rat medial habenula neurons. *J Neurophysiol* **74:**195–206.
Lewis TM, Harkness PC, Sivilotti LG, Colquhoun D and Millar NS (1997) The ion channel properties of rat recombinant neuronal nicotinic receptor are dependent on the host cell type. *J Physiol* **505:**299–306.
Lindstrom J (1995) Nicotinic acetylcholine receptors, in *Ligand- and Voltage-Gated Ion Channels* (North RA, ed) pp 153–175, CRC, Boca Raton, FL.
Lindstrom J (1996) Neuronal nicotinic acetylcholine receptors, in *Ion Channels*, vol. 4 (Narahashi T ed) pp 377–450, Plenum Press, New York.
Luetje CW and Patrick J (1991) Both α- and β-subunits contribute to the agonist sensitivity of neuronal nicotinic acetylcholine receptors. *J Neurosci* **11:**837–845.
Maconochie DJ and Steinbach JH (1998) The channel opening rate of adult- and fetal-type mouse muscle nicotinic receptors activated by acetylcholine. *J Physiol* **506:**53–72.
Mathie A, Colquhoun D and Cull-Candy SG (1990) Rectification of currents activated by nicotinic acetylcholine receptors in rat sympathetic ganglion neurons. *J Physiol* **427:**625–655.
McGehee DS and Role LW (1995) Physiological diversity of nicotinic acetylcholine receptors expressed by vertebrate neurons. *Annu Rev Physiol* **57:**521–546.
Mulle C, Choquet D, Korn H and Changeux JP (1992) Calcium influx through nicotinic receptor in rat central neurons: Its relevance to cellular regulation. *Neuron* **8:**135–143.
Nooney JM and Feltz A (1995) Inhibition by cyclothiazide of neuronal nicotinic responses in bovine chromaffin cells. *Br J Pharmacol* **114:**648–655.
Nooney JM, Peters JA and Lambert JJ (1992) A patch clamp study of the nicotinic acetylcholine receptor of bovine adrenomedullary chromaffin cells in culture. *J Physiol* **455:**503–527.
Séguéla P, Wadiche J, Dineley-Miller K, Dani JA and Patrick J (1993) Molecular cloning, functional properties, and distribution of rat brain α7: A nicotinic cation channel highly permeable to calcium. *J Neurosci* **13:**596–604.
Sine SM and Steinbach JH (1984) Agonists block currents through acetylcholine receptor channels. *Biophys J* **46:**277–283.
Stauderman KA, Mahaffy LS, Akong M, Velicelebi G, Chavez-Noriega LE, Crona JH, Johnson EC, Elliott KJ, Gillespie A, Reid RT, Adams P, Harpold MM and Corey-Naeve J (1998) Characterization of human recombinant neuronal nicotinic acetylcholine receptor subunit combinations α2β4, α3β4 and α4β4 stably expressed in HEK293 cells. *J Pharmacol Exp Ther* **284:**777–789.
Stetzer E, Ebbinghaus U, Storch A, Poteur L, Schrattenholz A, Kramer G, Methfessel C and Maelicke A (1996) Stable expression in HEK-293 cells of the rat α3/β4 subtype of neuronal nicotinic acetylcholine receptor. *FEBS Lett* **397:**39–44.
Tang C-M, Dichter M and Morad M (1989) Quisqualate activates a rapidly inactivating high conductance ionic channel in hippocampal neurons. *Science (Wash DC)* **243:**1474–1477.
Vernino S, Amador M, Luetje CW, Patrick J and Dani JA (1992) Calcium modulation and high calcium permeability of neuronal acetylcholine receptors. *Neuron* **8:**127–134.
Wada K, Ballivet M, Boulter J, Connolly JG, Wada E, Deneris ES, Swanson LW, Heinemann S and Patrick J (1988) Functional expression of a new pharmacological subunit of brain acetylcholine receptor. *Science (Wash DC)* **240:**330–334.
Wong ET, Holstad SG, Mennerick SJ, Hong SE, Zorumski CF and Isenberg KE (1995) Pharmacological and physiological properties of putative ganglionic nicotinic receptor, $\alpha_3\beta_4$, expressed in transfected eukaryotic cells. *Mol Brain Res* **28:**101–109.
Xiao Y, Meyer EL, Thompson JM, Surin A, Wroblewski J and Kellar KJ (1998) Rat α3/β4 subtype of neuronal nicotinic acetylcholine receptor stably expressed in a transfected cell line: Pharmacology of ligand binding and function. *Mol Pharmacol* **54:**322–333.

Send reprint requests to: Dr. Martin Morad, Georgetown University Medical Center, Department of Pharmacology, 3900 Reservoir Road N.W., Washington, DC 20007. E-mail: moradm@gunet.georgetown.edu